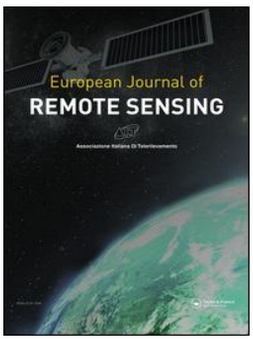

European Journal of Remote Sensing

ISSN: (Print) 2279-7254 (Online) Journal homepage: http://www.tandfonline.com/loi/tejr20

Analysis of two years of ASCAT-and SMOS-derived soil moisture estimates over Europe and North Africa

Nazzareno Pierdicca, Luca Pulvirenti, Fabio Fascetti, Raffaele Crapolicchio & Marco Talone

To cite this article: Nazzareno Pierdicca, Luca Pulvirenti, Fabio Fascetti, Raffaele Crapolicchio & Marco Talone (2013) Analysis of two years of ASCAT-and SMOS-derived soil moisture estimates over Europe and North Africa, European Journal of Remote Sensing, 46:1, 759-773, DOI: 10.5721/EuJRS20134645

To link to this article: http://dx.doi.org/10.5721/EuJRS20134645

Published online: 17 Feb 2017.

European Journal of Remote Sensing - 2013, 46: 759-773
doi: 10.5721/EuJRS20134645
Received 15/02/2013, accepted 01/10/2013

European Journal of Remote Sensing
An official journal of the Italian Society of Remote Sensing

www.aitjournal.com

Analysis of two years of ASCAT- and SMOS-derived soil moisture estimates over Europe and North Africa

Nazzareno Pierdicca[1], Luca Pulvirenti[1], Fabio Fascetti[1]*, Raffaele Crapolicchio[2,3] and Marco Talone[2]

[1]Department of Information Engineering Electronics and Telecommunications, Sapienza Univ. of Rome (Italy), via Eudossiana 18, 00194 – Rome, Italy
[2]Serco SpA, via Sciadonna 24/26, 00044 – Frascati, Italy
[3]ESA-ESRIN, via Galileo Galilei, 00044 – Frascati, Italy
*Corresponding author, e-mail address: fabiofasc@virgilio.it

Abstract

More than two years of soil moisture data derived from the Advanced SCATterometer (ASCAT) and from the Soil Moisture and Ocean Salinity (SMOS) radiometer are analysed and compared. The comparison has been performed within the framework of an activity aiming at validating the EUMETSAT Hydrology Satellite Application Facility (H-SAF) soil moisture product derived from ASCAT. The available database covers a large part of the SMOS mission lifetime (2010, 2011 and partially 2012) and both Europe and North Africa are considered. A specific strategy has been set up in order to enable the comparison between products representing a volumetric soil moisture content, as those derived from SMOS, and a relative saturation index, as those derived from ASCAT. Results demonstrate that the two products show a fairly good degree of correlation. Their consistency has some dependence on season, geographical zone and surface land cover. Additional factors, such as spatial property features, are also preliminary investigated.

Keywords: Remote sensing, SMOS, ASCAT, soil moisture.

Introduction

The role of soil moisture as a key variable for the characterization of the global climate is widely recognized within the international scientific community. The importance of its monitoring stems from the fact that it influences the water cycle by controlling the partition of rainfall between land (infiltration, percolation and runoff) and the atmosphere (evaporation and plant transpiration). Its knowledge is therefore essential for several applications, such as drought and flood predictions, meteorology, agronomy and climatology. Soil moisture maps at different spatial scales are currently assimilated within hydrological models [e.g. Brocca et al., 2012], or used as realistic initial states by numerical weather prediction (NWP) models [e.g. Panegrossi et al., 2011]; they are also used by models of carbon fluxes and plant growth [e.g. Lehuger et al., 2009].

Although soil moisture can be accurately monitored using in situ measurement techniques [Walker et al., 2004a], the small number of soil moisture networks available in the world implies that only satellite remote sensing allows for attaining at the same time satisfactory sampling frequency and global coverage. In particular, remote sensing measurements exhibit a direct sensitivity to the Soil Moisture Content (*SMC*) at microwave bands, where *SMC* influences the soil electrical permittivity, and the atmosphere can be considered as fairly transparent.

Microwave remote sensing encompasses both active and passive forms, depending on the sensor and its mode of operation. Passive sensors (radiometers) detect the naturally emitted microwave radiation within their field of view; the spatial resolution is in the order of a few tens of kilometres in order to detect sufficient energy to record the signal. Active microwave sensors provide their own source of energy and basically measure the ratio (in terms of power density) between the transmitted and received electromagnetic radiation (i.e., the radar backscattering coefficient). Among active sensors, scatterometers, which are primarily used to obtain information on wind speed and direction over ocean, offer the opportunity to achieve revisit time consistent with the requirements of a soil moisture product (in the order of five days, or less, see [Walker et al., 2004b]), although their spatial resolution is similar to that of microwave radiometers. However, it is worth underlining that in the near future even Synthetic Aperture Radars (SARs), which allow for the generation of *SMC* maps with a spatial resolution in the order of hundreds of meters, will offer revisit times in the order of six days (or less, in Europe and Canada, see [Hornáček et al., 2012; Pierdicca et al., 2013a], thanks to the forthcoming Sentinel-1 mission.

Sensors operating at C-band turned out to be useful for *SMC* mapping; in particular, sensitivity to *SMC* was demonstrated by the Advanced Microwave Scanning Radiometer on Earth Observing System (AMSR-E) aboard the AQUA satellite [e.g. Gruhier et al., 2010] and by active instruments, such as the scatterometer onboard ERS [Wagner et al., 1999], as well as by the ENVISAT/Advanced Synthetic Aperture Radar (ASAR) [Mattia et al., 2006; Pathe et al., 2007; Paloscia et al., 2008; Pierdicca et al., 2013b]. A great potential is offered by polarimetric sensors, as demonstrated by the Airborne Synthetic Aperture Radar (AirSAR) [Pierdicca et al., 2010] and the SIR-C radar [Pierdicca et al., 2008a]. It is well-known that L-band (~1.4 GHz) is the optimal spectral range to observe soil moisture because of its large penetration into the soil and its low sensitivity to the overlaying vegetation; moreover, passive measurements are also less sensitive to soil roughness than backscattering data. Consequently, the first spaceborne mission carrying a microwave radiometer designed for soil moisture, i.e., the European Space Agency (ESA) Soil Moisture and Ocean Salinity (SMOS) satellite [Kerr et al., 2001], launched in 2009, uses an L-band interferometric radiometer (MIRAS). Two L-band instruments, i.e., a passive radiometer and an active radar, are presently on board the Aquarius SAC-D satellite; even the future Soil Moisture Active and Passive (SMAP) mission will host a radiometer and a radar working at L-band.

The European Organisation for the Exploitation of Meteorological Satellites (EUMETSAT) Satellite Application Facility (SAF) on support to operational hydrology and water management (H-SAF) was established by the EUMETSAT council in July 2005. The objective is the provision of new satellite-derived products for use in operational hydrology, as well as the independent assessment (or validation) of the benefit of the new products for hydrological applications (see www.eumetsat.int). Within the framework of the H-SAF project, an activity consisting of the validation of the soil moisture H-SAF product, which

is derived from the C-band data of the Advanced SCATterometer (ASCAT) on board the MetOp satellite, is presently accomplished. Different institutions in Europe are involved in this task, coordinated by the Italian Department of Civil Protection. Many efforts are devoted to the comparison with reference in situ data, but considering the limitations of the presently available networks previously pointed out, this is a challenging task, especially at continental scale, as in the case of EUMETSAT H-SAF data. A possible choice is to assess the ASCAT soil moisture through a comparison with retrievals from an instrument designed for *SMC* applications, such as SMOS. When comparing *SMC* estimates from active and passive microwave instruments it must be considered that although surface emission and radar backscattering are in some way linked, being sensitive to common parameters, such as soil permittivity, roughness and vegetation conditions, their relationships with *SMC* are not identical. In fact, emissivity is related to the integral of the bistatic scattering coefficient over the upper hemisphere, thus accounting for the sensitivity to *SMC* of all the possible bistatic radar configurations [Pierdicca et al., 2008b], whereas a spaceborne scatterometer is monostatic.

In the literature, some studies comparing SMOS and ASCAT *SMC* are available. Albergel et al. [2012] analysed ASCAT and SMOS data, together with the outputs of the ECMWF (European Centre for Medium-Range Weather Forecasts) NWP model, through a comparison with in-situ data from stations located in Africa, Australia, Europe and United States over the year 2010. ASCAT and SMOS exhibited a correlation coefficient with in-situ soil moisture in the order of 0.55. It was found that SMOS performances have a weaker dependence on seasons than ASCAT, probably because of the less sensitivity of L-band to vegetation with respect to C-Band.

Leroux et al. [2013] compared ASCAT, SMOS, AMSR-E and ECMWF soil moisture maps for the year 2010 over four watersheds located in the United States with different soil characteristics. While ASCAT was scaled to the in situ measurements, and then considered in the analysis only for the correlation coefficient, SMOS retrievals presented the lowest bias among the other maps with respect to in-situ measurements, with an average of 0.032 m^3/m^3 and the lowest root mean square error over all sites except one. Moreover, a difference between morning and afternoon products was found, showing better scores in the morning.

Parrens et al. [2012] carried out a comparison between SMOS and ASCAT soil moisture products both with in-situ observations in southern France and land surface model simulations over the whole of France. Consistent results were found in wet conditions, while several differences were evidenced due to topography or other geographical factors (finding that the ASCAT *SMC* outperformed the SMOS product).

SMC derived from radiometers and scatterometers were compared also by Rüdiger et al. [2009] and Brocca et al. [2011]. In the former paper, an intercomparison of ERS Scatterometer and AMSR-E soil moisture observations with model simulations over France was accomplished. It was found that the ERS product was less influenced by the forest cover with respect to the passive retrievals, when considering the AMSR-E radiometer data at C- and X-bands. Brocca et al. [2011] compared *SMC* estimations through ASCAT and AMSR-E sensors by considering 17 sites located in Italy, Spain, France and Luxembourg. Their analysis showed that, considering relative soil moisture values for a 5 cm soil layer, the ASCAT product outperformed AMSR-E in France and central Italy, while similar results were obtained in the other regions.

Within the framework of the soil moisture H-SAF product validation activity, an extensive comparison between the H-SAF soil moisture estimated from ASCAT and that retrieved from SMOS has been carried out and its preliminary outcomes are presented in this study. The analysis is performed over the whole Europe and North Africa considering the years 2010, 2011 and the first three months of 2012. Note that after March 2012 the processor producing SMOS *SMC* has been modified, so that we have not considered later SMOS data to avoid analysing inconsistent retrievals. Our analysis demonstrates that the two different estimates present a fairly good degree of correlation (close to 0.7); it has also highlighted that the result of the comparison partially depends on factors such as geographical area, season and, as expected, land cover.

The soil moisture data and the comparison approach

ASCAT is a radar instrument that operates at C-band in vertical polarization and measures the radar backscatter [Bartalis et al., 2007]. Measurements are taken on both sides of the sub-satellite track over two 550 km wide swaths, from a 817 Km height orbit; there are 14 orbit revolutions per day resulting in a global coverage achieved in ~1.5 days. The H07 SM-OBS-1 product, available through the EUMETSAT H-SAF project, has been used for the comparison; it has a spatial resolution of 25 km and is resampled to a 12.5 km grid. It is generated by means of an algorithm originally conceived, at the Vienna University of Technology, for the ERS scatterometer [Wagner et al., 1999]. The algorithm is based on a change detection approach which assumes that soil moisture is linearly related to backscattering (in dB units) and that the temporal changes of surface roughness, canopy structure and vegetation biomass occur at longer temporal scales than soil moisture changes, so that *SMC* variations in time can be detected. As a matter of fact, for each SM-OBS-1 map, a pixel value represents a relative value (soil moisture index between 0% and 100%) of moisture with respect to the driest and wettest conditions registered for that pixel during the calibration phase of the algorithm. Note that this change detection approach is an empirical approach looking at the difference in soil moisture content as function of time. Other multitemporal approaches proposed in the literature, based on similar hypothesis, invert an electromagnetic forward model [see for instance Pierdicca et al., 2010; Balenzano et al., 2011]; the latter method may in principle provide estimates of SMC in m^3/m^3. In general, there are strengths and weaknesses associated to a purely theoretical approach and a change detection technique, whose discussion is beyond the scope of this work, but can be found for instance in Pierdicca et al. [2013a].

MIRAS-SMOS is an interferometric radiometer that measures the cross correlations between pairs of receivers to derive a visibility function. The surface emission is related to the inverse Fourier transform of this function [Parrens et al., 2012] and is measured at several incidence angles, for two polarizations. SMOS operates at 1.427 GHz (L-band) from a 758 height orbit with a repetition time of 3 days and a spatial resolution of about 35 km. The reprocessed L2 product that provides an actual volumetric moisture content (see the SMOS Level 2 and Auxiliary Data Products Specifications, 2012, available at https://earth.esa.int) has been used; the version number of the processor is 501. L2 data are sampled over the ISEA4h9 grid, which has a spacing in the order of 15 km [Kidd, 2005]. It is worth underlining that the SMOS signal can be perturbed by Radio Frequency Interferences (RFI) and the SMOS L2 processing filters out the data strongly affected by RFI, i.e., only those for which RFI is such to produce outliers.

A large database of pairs of ASCAT- and SMOS- derived soil moisture estimates (also indicated as SMI_{ASCAT} and SMC_{SMOS}, respectively), over Europe and North Africa, has been built in order to perform an extensive comparison between the two products. For this purpose, ASCAT and SMOS estimates have been co-located in space and time. Firstly, for each SMOS grid point, the closest ASCAT grid point has been searched for (i.e., a nearest neighbour approach has been adopted); the left panel of Figure 1 shows the histogram of the distance between co-located ASCAT and SMOS grid points, which has the most probable value equal to 6.7 km and the largest one equal to ~9 km. Then, to minimize the temporal mismatch between daily SMOS and ASCAT data, only the orbits closest in time have been considered; hence, the SMOS ascending (descending) orbits and the ASCAT descending (ascending) orbits have been combined, as shown in the right panel of Figure 1. It can be noted that the time difference is in the range between 0 and 6.6 hours with the most probable value in the order of 200 minutes.

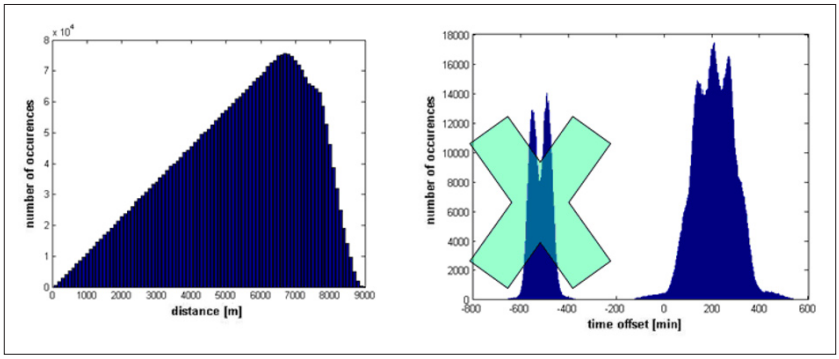

Figure 1 - Histograms of the spatial (left panel) and temporal (right panel) distances between co-located ASCAT and SMOS grid points. Data under the X sign have been discarded, because they represent combinations of SMOS - ASCAT ascending orbits and SMOS - ASCAT descending orbits, that have a large temporal mismatch.

The fact that ASCAT product is actually an index (in the range 0-100), in contrast with SMOS absolute estimates (in m^3/m^3) represents a critical aspect of this comparison, which requires to express in some way the two moisture products by the same unit of measurement. Hence, the SMI_{ASCAT} has been converted into a volumetric moisture in m^3/m^3 considering that, by definition, it represents the distance of each resolution cell from its driest and wetter soil condition. In principle, this conversion could be performed through the soil porosity. However, although information on soil porosity can be derived from soil maps, such data are not available at a global scale and existing maps are often not very accurate [Brocca et al., 2011]. Consequently, in the literature, methods such as assigning the same maximum and minimum *SMC* values to each grid point [e.g. Leroux et al., 2013], or fixing the same mean and standard deviation values [e.g. Dorigo et al., 2010] have been used to rescale ASCAT data. Another relevant point concerns the dataset used for the normalization; often it is the set of co-located data, but in this case a limited database and/or a limited timeframe might be considered. The normalization can be also based

on a larger set of data (i.e., not only those co-located with ASCAT, but all the available ones), or even on independent data (i.e., data not used for the purpose of the comparison). The former approaches tend to improve the agreement between the compared data, whilst the latter ones can be considered as more conservative.

In this work, maps of the maximum and minimum *SMC* values estimated from all the available SMOS L2 data collected throughout the period January 2010 - March 2012 (i.e., not only those co-located with ASCAT) have been produced, denoted as $\max(SMC_{SMOS})$ and $\min(SMC_{SMOS})$, respectively. The maximum value is actually computed as the value above which the percentage of occurrences of the data is 1% (i.e., we have disregarded the last percentile), and the same approach has been carried out for estimating the minimum (i.e., the first percentile has been also disregarded); this has been done to avoid including possible outliers (i.e., unreasonably low or large values of soil moisture) in the computation of $\max(SMC_{SMOS})$ and $\min(SMC_{SMOS})$. Both ascending and descending orbits have been considered to compute the maps that are shown in Figure 2.

Looking at Figure 2, it can be noted that, in the coastal areas of North Africa, Spain, Netherlands and Belgium, as well as over Ireland, large values of $\max(SMC_{SMOS})$ have been found; smallest values are observed in the desert, as expected, whereas the map of $\min(SMC_{SMOS})$ is quite uniform. Note that these maps have been computed by considering only grid points with significant statistics, i.e., where the number of observations is greater than 50, and a minimum number of 6 observations in Summer, Spring and Autumn is available. Lack of data and points exhibiting doubtful estimates of $\max(SMC_{SMOS})$ are apparent in Figure 2, which are likely due to the scarcity of available SMOS data for different reasons (snow/ice cover, topography, RFI and so on). This should be considered in the comparison presented in the following sections.

For each SMOS grid point, the co-located SMI_{ASCAT} has been converted into an absolute value of *SMC* through the following linear transformation:

$$\frac{SMC_{ASCAT} - \min\left(SMC_{SMOS}\right)}{\max\left(SMC_{SMOS}\right) - \min\left(SMC_{SMOS}\right)} = \frac{SMI_{ASCAT}}{100} \quad [1]$$

According to equation [1] and to the definition of SMI_{ASCAT}, $\min(SMC_{SMOS})$ and $\max(SMC_{SMOS})$ are assigned to the driest (SMI_{ASCAT}=0) and wettest (SMI_{ASCAT}=100) conditions, that is, they are used as calibrations points for the conversion of ASCAT data into volumetric moisture. Note that a perfectly equivalent approach could consist in scaling the SMC_{SMOS} into a relative quantity using their own minimum and maximum values.

Considering that, as previously underlined, the reliability of some estimates of $\max(SMC_{SMOS})$ can be questioned, the results of the comparison between ASCAT and SMOS products has been also evaluated by considering two additional normalization approaches (see the following section): *i*) rescaling of the ASCAT data according to the average and the variance of the SMOS *SMC* values of each pixel by using the co-located dataset; *ii*) use of independent minimum and maximum soil moisture maps, as those available from the NOAA (National Oceanic and Atmospheric Administration) website. Note that the latter data are represented on a T62 Gaussian grid with 192×94 points (88.542N-88.542S, 0E-358.125E), so that they have been resampled on the SMOS isea4h9 grid.

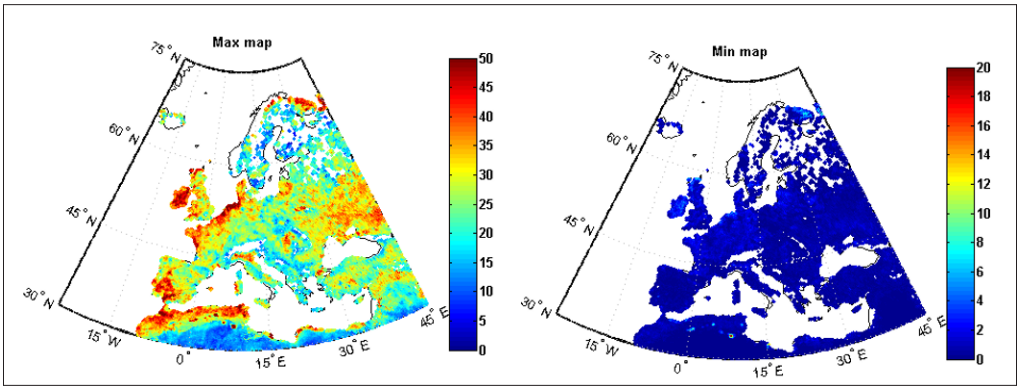

Figure 2 - Maps of maximum (left) and minimum (right) SMOS SMC (expressed in percentage of volumetric soil moisture, 100*m3/m3) for the period January 2010 - March 2012 in the study area over Europe and Northern Africa.

After co-locating SMOS and ASCAT data in time and space and rescaling the relative SMI_{ASCAT} to *SMC* values, we have selected the data fulfilling the following conditions: 1) SMOS retrievals with Data Quality Index (*DQX*) less than 0.045 (for details on how this index is computed the reader may refer to the SMOS documentation); 2) ASCAT retrievals with less than 4 bad quality flags up. Through this quality control, a data base of 3589584 records has been attained.

Results and discussion

Figure 3 shows the result of the comparison between SMC_{ASCAT} and SMC_{SMOS} values in the form of a scatterplot, while the first line of Table 1 reports the main statistical scores describing the matching between the two products, namely the correlation coefficient (*R*), the root mean square difference (*RMSD*), the bias (*B*), and the slope (*S*) of the best fit line (red in Fig. 3). A fairly good correlation (R=0.67) and a small bias between the two products can be observed, although the points are quite scattered so that the *RMSD* exceeds 7%. The large value of *S* (0.78) demonstrates that, in general, the variations of SMC_{SMOS} are detected by ASCAT (and vice versa).

As mentioned in the previous section, to rescale ASCAT data, other two methods have been applied to verify the impact of different normalization methods on the results of the comparison. By fixing the same mean and standard deviation values of *SMC* for each point grid, *R* does not substantially change while, as expected since the co-located set of data has been used in this case, *RMSD* drops off to 6.3%. Conversely, by using the NOAA maps of maximum and minimum *SMC*, the results tend to worsen (R~0.56 and *RMSD* ~17%, mainly because *B* is in the order of 14%). A further verification of the generality of our results has been carried out by changing the co-location method. For this purpose, we have integrated ASCAT data within each SMOS pixel, instead of using the nearest neighbour, by linearly combining them according to their inverse distance from the SMOS grid point. Also in this case, the results are substantially the same since the distance between pixel centres is in the order of 6-7 km (see the left panel of Fig. 1), so that in most cases, there is a large overlapping between a SMOS pixel and the nearest ASCAT one.

The previous outcomes are quite general since the data are considered all together. However, when cross-validating different products over a continental scale it is also interesting to analyse the result attained in different regions of the continent and in different seasons.

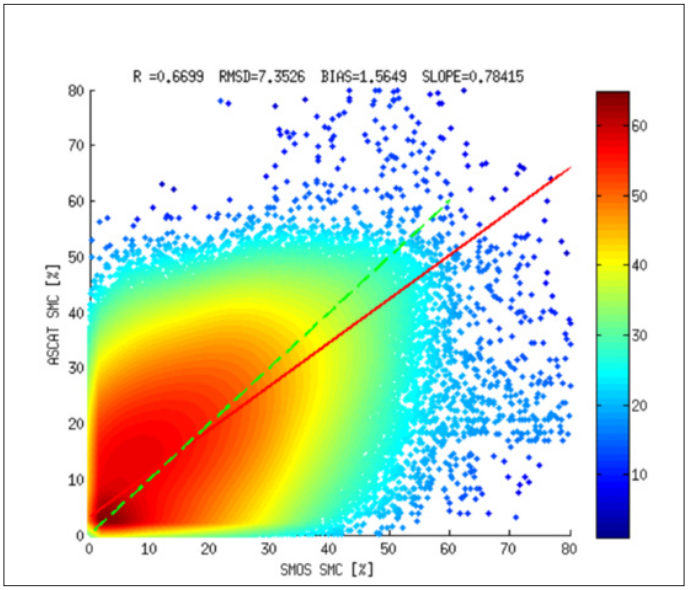

Figure 3 - SMOS SMC versus co-located H-SAF SMC (after the conversion of the latter into absolute volumetric soil moisture). The red line represents the best fit, while the different colours represent the points density in the scatterplot.

Table 1 - Statistical scores (Root Mean Square Difference, Correlation Coefficient, Bias, Slope of Fitting line) of the comparison between ASCAT and SMOS derived SMC products evaluated in different geographic areas.

	R [#]	RMSD [%]	BIAS [%]	SLOPE [#]	nRECORD
All Data	0.67	7.3	1.6	0.78	3589584
North Africa	0.65	4.3	-1.1	0.54	1410898
Western Europe	0.50	9.0	2.3	0.53	853761
Eastern Europe	0.49	9.5	5.5	0.50	931966

Table 1 reports the statistical scores obtained by separately considering three different macro-regions (Western Europe, Eastern Europe and Northern Africa). The results show a better agreement in Northern Africa, where a stable soil moisture spatial pattern, from the dry desert to coastal areas, is present. The scores in Table 1 account for both the spatial and the temporal variability of the two data sets, so that the temporal stability of the spatial patterns of soil moisture, as well as the high dynamic between the coastal area and the desert area contribute to the result over North Africa. The worst results have been obtained in Eastern Europe where, although the temporal correlation between SMC_{ASCAT} and SMC_{SMOS} is quite high (see Fig.

5, commented in the sequel) the spatial correlation is not so high and *R* is less than 0.5. In other words, both sensors have detected the same temporal variability, likely associated to the seasonal variability and the precipitations events, but the presence of forests and snow/ice has probably produced a different spatial noisy signal in the maps, also considering the different effects that these two types of coverage have on the two sensors.

Besides the geographic area, also the season is expected to influence the results of the comparison between SMC_{ASCAT} and SMC_{SMOS}. The values of *R* and *RMSD* computed for the four seasons are shown in Figure 4 (see the blue lines). It can be noted that the best results have been obtained in winter; *R* is high in autumn too, while the smallest *R* and the highest *RMSD* have been obtained in summer. This is probably due to the large scale spatial variability and short term temporal variability of *SMC* in winter, which have been reliably detected by both sensors, whereas in summer, when *SMC* is generally low and varies on a smaller scale, especially in Southern Europe and Northern Africa, detecting changes has turned out to be difficult for both sensors. Finally, we have analysed also the influence of land cover, since it is well-known that over vegetated/forested areas *SMC* retrievals are very critical. It has been found that, as expected, by discarding the retrievals over pixels labelled as covered by forest in the SMOS L2 product, the evaluation scores significantly improve, as it can be seen by looking at Table 2 (first two rows) and at Figure 4 (red lines).

Table 2 - Influence of land cover and of the proposed relative DQX (RDQX) on the scores evaluating the comparison between ASCAT and SMOS derived SMC products.

	R [#]	RMSD [%]	BIAS [#]	SLOPE [#]	nRECORD
All Data	0.67	7.3	1.2	0.78	3589584
No Forest	0.72	6.5	0.4	0.583	2512780
All Data RDQX<0.12	0.79	7.0	-1.1	0.89	1220496
No Forest RDQX<0.12	0.79	6.7	-1.5	0.89	1050117

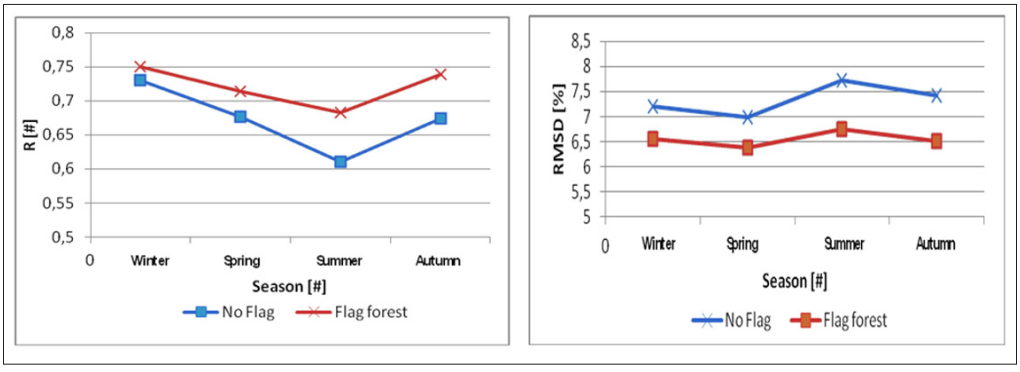

Figure 4 - Seasonal values of the correlation coefficient (left panel) between ASCAT and SMOS SMC and of the root mean square difference (right panel). For the red lines areas labelled as forests by the SMOS L2 product have been flagged out.

The previous results have been obtained by performing a data quality control based on the quality flags of the SM-OBS-1 product and on the *SMC DQX* available from the SMOS L2

product. However, it is worth verifying whether an improvement of the results of the comparison can be obtained through a more careful selection of the data to be compared. It has been found that the results improve if, instead of using a threshold on the *DQX* (a value of 0.045 has been used, as previously mentioned), the *SMC* data are filtered based on the ratio between *DQX* and SMC_{SMOS} (i.e., a sort of relative *SMC DQX*, hereafter denoted as *RDQX*). The last two rows of Table 2 report the results obtained by discarding *RDQX*>0.12; this threshold value, after performing various tests, has turned out to be the best compromise between the improvement of the evaluation scores and an excessive masking of the *SMC* data. In fact the *DQX* tends to be proportional to the estimated *SMC*, so that the threshold on the *DQX* tends to mask lower values of *SMC*, despite of their actual reliability. It is worth pointing out that 77% of grid points whose *RDQX* is always above the threshold are labelled as forests by the flag included in the SMOS L2 product. This finding can be considered as a proof of the utility of the proposed index, because it demonstrates that *RDQX* is capable to filter out unreliable data as those collected over forested areas, even without any prior information on the location of forests.

As soil moisture is a function of both space and time, it is interesting to try to single out the capability of both instruments to detect both time evolution and spatial patterns. As for the temporal evolution, a map representing, pixel by pixel, the temporal correlation between SMC_{ASCAT} and SMC_{SMOS} has been produced and is shown in Figure 5. It is worth underlining that the transformation that has been carried out for comparing SMC_{ASCAT} and SMC_{SMOS} influences both *B* and *RMSD* at pixel scale, whilst *R* is invariant with respect to such a transformation. Moreover, considering that H-SAF products are intended to be assimilated into rainfall-runoff models, reproducing the temporal trend of soil moisture in each point is essential [Brocca et al., 2012]. For these reasons *R* likely represents the best indicator to assess the consistency between the two datasets. Note that the *R* map shown in Figure 5 has been produced by including only the grid points where at least more than 20 observations are available during the whole period under investigation.

Looking at Figure 5, it can be seen that high temporal correlations have been obtained in several regions of Europe and North Africa, whereas a small correlation (even negative) has been obtained in the desert area of North Africa, where the range of moisture variability is very small and the behaviour of the two instruments is quite incoherent, probably because of the higher and different penetration depth between C- and L-band radiations in the presence of a dry sand. Unfortunately, in the desert area, in situ data are almost completely unavailable so that it was unfeasible at the moment to investigate in detail this quite surprising finding, which has already been observed before [e.g. de Jeu et al., 2008]. Except for the desert area, the results demonstrate that almost all over Europe and North Africa the *SMC* estimates derived from SMOS and ASCAT are consistent. Less agreement can apparently be associated to areas with complex topography and possibly affected by permanent snow cover or frozen soil. Undetected RFI effects (we remind that the SMOS L2 processing filters out the data for which RFI is such to produce outliers) could also be responsible of the mismatches in some cases.

Another interesting comparison concerns the spatial variability of soil moisture as estimated by the two sensors. We have computed the correlation coefficient between the daily co-located SMC_{ASCAT} and SMC_{SMOS}, in order to verify the agreement of the spatial patterns. The result is reported in Figure 6 as function of time (day of the year: doy) for years 2010 and 2011 (considering that only 3 months are analysed for 2012). Although the correlation coefficient as function of time is quite scattered (note that the co-located maps may refer to different geographic

areas in different days), it is possible to note again that winter and autumn are the seasons when the spatial patterns present the greatest agreement. Moreover, for each year, the trend is quite similar except for some sudden decreases of *R* around doy 45 in 2011 and doy 120 in 2010.

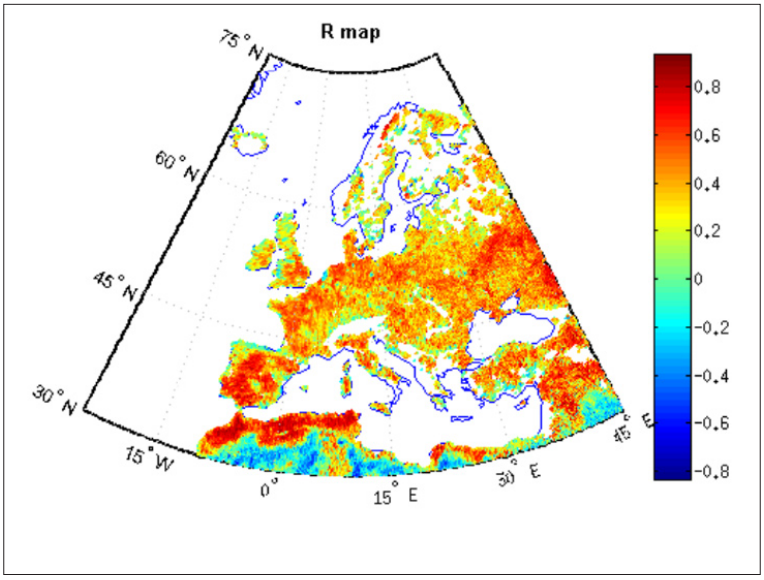

Figure 5 - Map of the correlation coefficient (R) between ASCAT and SMOS soil moisture retrievals.

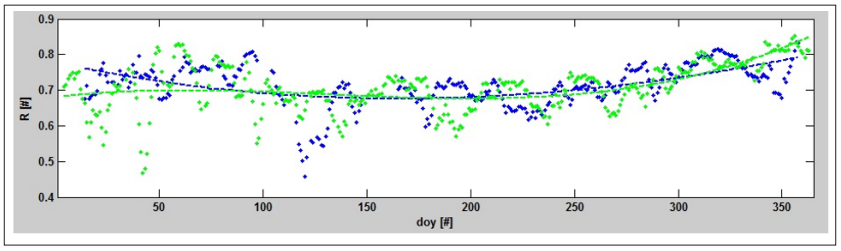

Figure 6 - Spatial correlation coefficient (R) between the ASCAT and SMOS retrievals as function of the day of the year (doy) for years 2010 (blues) and 2011 (green).

Another promising approach to analyse the capability to reproduce the spatial patterns, which is preliminarily exploited in this paper, can be based on the semivariogram geostatistical approach. As an example, a comparison between SMOS and ASCAT isotropic semivariograms is shown in Figure 7. The semivariogram is computed as a "mean" semivariogram over all the days of the comparison, that is the variance of each increment (i.e., corresponding to each lag) is the average of the variances computed for that lag in the different days. We have limited the geographical area considered to compute

the semivariogram removing the data over Africa, in order to retain a region where the soil moisture can be reasonably considered an intrinsic second order stationary process (avoiding the very low mean values over the desert). The semivariogram provides some insights on the spatial characteristics of the maps. Making reference for instance to the discussion in Montopoli et al. [2012], we can observe that SMOS has a slightly larger variability for small spatial scales (lag < 200 km). The discontinuity of the semivariogram between lag=0 (where it is by definition equal to zero) and lag>0 is generally associated to the noise in the regionalized variable (i.e., the nudget). However, the noise would also contribute to the global variance, which is quite similar between SMOS and ASCAT (it corresponds to the limit of the semivariogram when lag goes to infinity). Finally, the slope of the increase for small lags can be associated to the correlation length, since the faster the increase, the steepest the decrease of the autocovariance function and thus the shorter the correlation length. In conclusion, although quite preliminary, this analysis would indicate a slightly better performances of the SMOS product in reproducing the small scale variability, although it is important to underline that the semivariogram depends strongly by the scaling approach. Since according to the intrinsic resolution of the instruments one should expect the opposite, this could be related to the way the data have been processed (e.g., the adopted interpolation algorithm), but further analysis is required to support this conclusion.

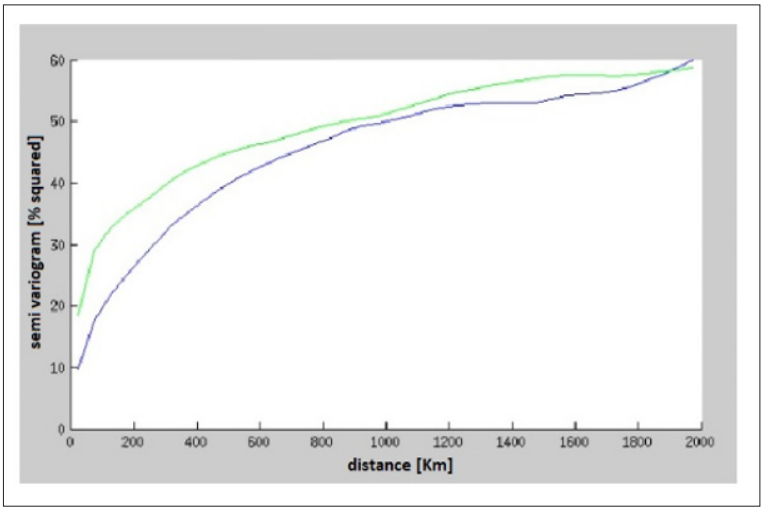

Figure 7 - Isotropic semivariogram, averaged over the considered satellite passes, of SMOS SMC maps (in green) and corresponding H-SAF SMC maps (in blue). Horizontal axis is space lag in km, whereas vertical axis is variance in % squared.

Conclusions

Within the framework of the H-SAF product validation activity, an extensive comparison between SMOS and ASCAT derived soil moisture retrievals has been carried out by considering the SM-OBS-1 ASCAT products and the SMOS L2 products. This comparison

aimed at assessing the consistency between SMOS and ASCAT retrievals, without establishing whether one product outperforms the other, since a third independent source providing the ground truth has not been considered yet. A very large dataset has been analyzed in order to improve the reliability of the outcomes. Both Europe and Northern Africa have been considered and data acquired during 2010, 2011 and the first three months of 2012 have been used. Results have demonstrated that the two products show an overall reasonable degree of correlation (0.67), together with a small bias (1.6%), while the root mean square difference exceeds 7%. However, the rescaling performed to compare soil moisture estimates, which has turned out to be the most critical aspect of this study, may influence these evaluation scores.

Surface factors, such as geographical area, season and land cover (especially the presence of forests) have been singled out to affect the consistency between SMOS and ASCAT, and more in general the quality of the soil moisture product the final user can expect. Moreover, a new SMOS data quality index, that is the ratio between the original SMOS data quality index and the SMOS-derived soil moisture content, has been proposed, whose consideration may lead to an increase of the agreement between ASCAT and SMOS. It has been also found that the spatial variability of the two estimates is more consistent in autumn and winter, whereas the temporal correlation has turned out to be poor in the desert areas of North Africa.

Future work will concern a deeper investigation of the semivariograms, and the assessment of the estimates by using ground data, as those belonging to the International Soil Moisture network, in the framework of the triple collocation approach.

Acknowledgments

SMOS L2 data have been gathered within the framework of an ESA category-1 project. ASCAT SM-OBS-1 data have been acquired within the H-SAF products validation activity. We would like to thank the Italian Department of Civil Protection, and especially Dr. Silvia Puca, for the support in this activity.

References

Albergel C., de Rosnay P., Gruhier C., Muñoz-Sabater J., Hasenauer S., Isaksen L., Kerr Y., Wagner W. (2012) - *Evaluation of remotely sensed and modelled soil moisture products using global ground-based in situ observations*. Remote Sensing of Environment, 118: 215-226. doi: http://dx.doi.org/10.1016/j.rse.2011.11.017.

Balenzano A., Mattia F., Satalino G., Davidson M.W.J. (2011) - *Dense Temporal Series of C- and L-band SAR Data for Soil Moisture Retrieval Over Agricultural Crops*. IEEE Journal of Selected Topics in Applied Earth Observations and Remote Sensing (JSTARS), 4 (2): 439-450. doi: http://dx.doi.org/10.1109/JSTARS.2010.2052916.

Bartalis Z., Wagner W., Naeimi V., Hasenauer S., Scipal K., Bonekamp H., Figa J., Anderson C. (2007) - *Initial soil moisture retrievals from the METOP-A advanced Scatterometer (ASCAT)*. Geophysical Research Letters, 34, L20401. doi: http://dx.doi.org/10.1029/2007GL031088.

Brocca L., Hasenauer S., Lacava T., Melone F., Moramarco T., Wagner W., Dorigo W., Matgen P., Martínez-Fernández J., Llorens P., Latron J., Martin C., Bittelli M. (2011) - *Soil moisture estimation through ASCAT and AMSR-E sensors: an intercomparison and validation study across Europe*. Remote Sensing of Environment, 115: 3390-3408. doi:

http://dx.doi.org/10.1016/j.rse.2011.08.003.

Brocca L., Moramarco T., Melone F., Wagner W., Hasenauer S., Hahn S. (2012) - *Assimilation of Surface- and Root-Zone ASCAT Soil Moisture Products Into Rainfall–Runoff Modeling*. IEEE Transactions on Geoscience and Remote Sensing, 50 (7): 2542 - 2555. doi: http://dx.doi.org/10.1109/TGRS.2011.2177468.

de Jeu R.A.M., Wagner W., Holmes T.R.H., Dolman A.J., van de Giesen N.C., Friesen J. (2008) - *Global Soil Moisture Patterns Observed By Space Borne Microwave Radiometers and Scatterometeters*. Surveys in Geophysics, 29:399-420. doi: http://dx.doi.org/10.1007/s10712-008-9044-0.

Dorigo W.A., Scipal K., Parinussa R.M., Liu Y.Y., Wagner W., de Jeu R.A.M., Naeimi V. (2010) - *Error characterisation of global active and passive microwave soil moisture datasets*. Hydrology and Earth System Sciences, 14: 2605-2616. doi: http://dx.doi.org/10.5194/hess-14-2605-2010.

Gruhier C., de Rosnay P., Hasenauer S., Holmes T., de Jeu R., Kerr Y., Mougin E., Njoku E., Timouk F., Wagner W., Zribi M. (2010) - *Soil moisture active and passive microwave products: intercomparison and evaluation over a Sahelian site*. Hydrology and Earth System Sciences, 14: 141-156. doi: http://dx.doi.org/10.5194/hess-14-141-2010.

Hornáček M., Wagner W., Sabel D., Truong H.-L., Snoeij P., Hahmann T., Diedrich E., Doubková M. (2012) - *Potential for High Resolution Systematic Global Surface Soil Moisture Retrieval via Change Detection Using Sentinel-1*. IEEE Journal of Selected Topics in Applied Earth Observations and Remote Sensing (JSTARS), 5 (4): 1303-1311. doi: http://dx.doi.org/10.1109/JSTARS.2012.2190136.

Kerr Y., Waldteufel P., Wigneron J.-P., Martinuzzi J.-M., Font J., Berger M. (2001) - *Soil Moisture retrieval from space: the Soil Moisture and Ocean Salinity (SMOS) mission*. IEEE Transactions on Geoscience and Remote Sensing, 39: 1729-1736. doi: http://dx.doi.org/10.1109/36.942551.

Kidd R.A. (2005) - *Implementation Plan for a NRT global ASCAT soil moisture product for NWP, Part 4: Discrete Global Grid Systems*. NWP SAF (Satellite Application Facility for Numerical Weather Prediction Associate Scientist Mission Report.

Lehuger S., Gabrielle B., van Oijen M., Makowski D., Germon J.-C., Morvan T., Hénault C. (2009) - *Bayesian calibration of the nitrous oxide emission module of an agro-ecosystem model*. Agriculture, Ecosystems & Environment, 133 (3-4): 208-222.

Leroux D.J., Kerr Y.H., Al Bitar A., Bindlish R., Jackson T.J., Berthelot B., Portet G. (2013) - *Comparison between SMOS, VUA, ASCAT, and ECMWF Soil Moisture Products Over Four Watersheds in U.S.* IEEE Transactions on Geoscience and Remote Sensing, in press. doi: http://dx.doi.org/10.1109/TGRS.2013.2252468.

Mattia F., Satalino G., Dente L., Pasquariello G. (2006) - *Using a priori information to improve soil moisture retrieval from ENVISAT* ASAR AP data in semiarid regions. IEEE Transactions on Geoscience and Remote Sensing, 44 (4): 900-912. doi: http://dx.doi.org/10.1109/TGRS.2005.863483.

Montopoli M., Pierdicca N., Marzano F.S. (2012) - *Spectral downscaling of integrated water vapor fields from satellite infrared observations*. IEEE Transactions on Geoscience and Remote Sensing, 50 (2): 415-428. doi: http://dx.doi.org/10.1109/TGRS.2011.2161996.

Paloscia S., Pampaloni P., Pettinato S., Santi E. (2008) - *A comparison of algorithms for retrieving soil moisture from ENVISAT/ASAR images*. IEEE Transactions on Geoscience and Remote

Sensing, 46 (10): 3274-3284. doi: http://dx.doi.org/10.1109/TGRS.2008.920370.

Panegrossi G., Ferretti R., Pulvirenti L., Pierdicca N. (2011) - *Impact of ASAR soil moisture data on the MM5 precipitation forecast for the Tanaro flood event of April 2009*. Natural Hazards and Earth System Sciences, 11: 3135-3149. doi: http://dx.doi.org/10.5194/nhess-11-3135-2011.

Parrens M., Zakharova E., Lafont S., Calvet J.-C., Kerr Y., Wagner W., Wigneron J.P. (2012) - *Comparing soil moisture retrievals from SMOS and ASCAT over France*. Hydrology and Earth System Sciences, 16: 423-440. doi: http://dx.doi.org/10.5194/hess-16-423-2012.

Pathe C., Wagner W., Sabel D., Doubkova M., Basara J.B. (2007) - *Using ENVISAT ASAR Global Mode Data for Surface Soil Moisture Retrieval Over Oklahoma, USA*. IEEE Transactions on Geoscience and Remote Sensing, 47 (2): 468-480. doi: http://dx.doi.org/10.1109/TGRS.2008.2004711.

Pierdicca N. Castracane P., Pulvirenti L. (2008a) - *Inversion of Electromagnetic Models for Bare Soil Parameter Estimation from Multifrequency Polarimetric SAR Data*. Sensors, 8: 8181-8200. doi: http://dx.doi.org/10.3390/s8128181.

Pierdicca N., Pulvirenti L., Ticconi F., Brogioni M. (2008b) - *Radar Bistatic Configurations for Soil Moisture Retrieval: A Simulation Study*. IEEE Transactions on Geoscience and Remote Sensing, 46 (18): 3252-3264. doi: http://dx.doi.org/10.1109/TGRS.2008.921495.

Pierdicca N., Pulvirenti L., Bignami C. (2010) - *Soil moisture estimation over vegetated terrains using multitemporal remote sensing data*. Remote Sensing of Environment, 114: 440-448. doi: http://dx.doi.org/10.1016/j.rse.2009.10.001.

Pierdicca N., Pulvirenti L., Pace G. (2013a) - *A Prototype Software Package to Retrieve Soil Moisture from Sentinel 1 Data by Using a Bayesian Multitemporal Algorithm*. IEEE Journal of Selected Topics in Applied Earth Observations and Remote Sensing (JSTARS), in press, doi: http://dx.doi.org/10.1109/JSTARS.2013.2257698.

Pierdicca N., Pulvirenti L., Bignami C., Ticconi F. (2013b) - *Monitoring soil moisture in an agricultural test site using SAR data: design and test of an operational procedure*. IEEE Journal of Selected Topics in Applied Earth Observations and Remote Sensing (JSTARS), in press. doi: http://dx.doi.org/10.1109/JSTARS.2012.2237162.

Rüdiger C., Calvet J.-C., Gruhier C., Holmes T.R.H., de Jeu R.A.M., Wagner W. (2009) - *An intercomparison of ERS-Scat and AMSRE soil moisture observations with model simulations over France*. Journal of Hydrometeorology, 10 (2): 431-447. doi: http://dx.doi.org/10.1175/2008JHM997.1.

Wagner W., Lemoine G., Rott H. (1999) - *A method for estimating soil moisture from ERS scatterometer and soil data – Empirical data and model results*. Remote Sensing of Environment, 70 (2): 191-207. doi: http://dx.doi.org/10.1016/S0034-4257(99)00036-X.

Walker J.P., Willgoose G.R., Kalma J.D. (2004a) - *In situ measurement of soil moisture: a comparison of techniques*. Journal of Hydrology, 293 (1-4): 85-99. doi: http://dx.doi.org/10.1016/j.jhydrol.2004.01.008.

Walker J.P., Houser P.R. (2004b) - *Requirements of a global near-surface soil moisture satellite mission: Accuracy, repeat time, and spatial resolution*. Advances in Water Resources, 27 (8): 785-801. doi: http://dx.doi.org/10.1016/j.advwatres.2004.05.006.